

phys. stat. sol. (b) **96**, 589 (1979)

Subject classification: 10.2 and 20.1; 22.5.3

*E.R.A. n° 14, Université de Nancy I¹⁾***Far-Infrared Absorption of $\text{BaF}_2:\text{Dy}^{3+}$ versus Concentration**

By

G. VILLERMAIN-LECOLIER, G. MORLOT, A. ROGER, and A. HADNI

In the $\text{BaF}_2:\text{Dy}^{3+}$ FIR spectrum the vibration frequencies of the interstitial compensation ion F_i is observed and the presence of some cluster types is revealed for concentrations equal to or higher than 0.4 mol%. A 125 cm^{-1} line is observed for the first time with Dy^{3+} . In $\text{BaF}_2:\text{Nd}^{3+}$ and $\text{BaF}_2:\text{Ho}^{3+}$ studies it is previously ascribed to the F_i vibration longitudinal mode in a trigonal site. Calculation gives 135 cm^{-1} for the transversal mode vibration; experimentally it is observed for the first time. The 42 cm^{-1} line previously ascribed to an electronic transition of Dy^{3+} in trigonal site disappears when the concentration increases.

Le spectre infrarouge lointain de $\text{BaF}_2:\text{Dy}^{3+}$ permet d'observer les fréquences de vibration de ion de compensation interstitiel F_i . Cette étude révèle la présence de plusieurs types de clusters pour des concentrations égales ou supérieures à 0,4 mol%. On observe pour la première fois avec le Dy^{3+} la raie à 125 cm^{-1} que nous avons précédemment attribuée dans le cas de Nd^{3+} et Ho^{3+} au mode longitudinal de la vibration de F_i dans un site trigonal. Un modèle laissait alors prévoir la fréquence du mode transversal à 135 cm^{-1} ; nous l'observons ici expérimentalement pour la première fois. La raie à 42 cm^{-1} précédemment attribuée à une transition électronique de Dy^{3+} en site trigonal disparaît quand la concentration augmente.

1. Introduction

In previous papers we have studied the far infrared absorption of barium fluoride and strontium fluoride doped with trivalent rare earth ions: R^{3+} ($\text{R}=\text{Nd}, \text{Pr}, \text{Sm}, \text{Tb}, \text{Dy}, \text{Ho}, \text{Er}$). The molar concentration was 0.2% [1, 2].

For $\text{BaF}_2:\text{R}^{3+}$ crystals, we observe a common absorption band at 131.5 cm^{-1} which shows exactly the same structure for all rare earth ions. The structure of this band is explained by localised vibrations of the compensating F^- ions in three different interstitial sites: cubic (131.5 cm^{-1}), tetragonal (75.5 and 158 cm^{-1}), and trigonal sites (125 cm^{-1}).

On one hand, the far infrared spectra of $\text{SrF}_2:\text{R}^{3+}$ show essentially two broad absorption bands around 90 and 159 cm^{-1} explained by vibrations of the compensating F^- ion in a tetragonal site, and a line appears around 138 cm^{-1} attributed to a cubic and trigonal sites for the heaviest rare earth ions. On the other hand, two other lines at 96 and 136 cm^{-1} are observed for all rare earth ions.

In this paper we study the influence of the rare earth concentration ($\text{R}=\text{Dy}^{3+}$) on the far infrared absorption spectra of $\text{BaF}_2:\text{R}^{3+}$, because we wanted to see if the infrared method enables us to observe clustered rare earth ions. Many studies of CaF_2 , BaF_2 , SrF_2 , and CdF_2 doped with R^{3+} ions have been reported from optical, ENDOR, and ESR methods, and they revealed the presence of clusters with high R^{3+} concentration [3 to 10].

Barium fluoride has the fluoride structure with O_h^5 space group symmetry. The R^{3+} ion can enter the lattice substitutionally at Ba^{2+} sites. Under the growth conditions described in [1], charge compensation is reached with interstitial F^- ions: F_i . At 0.2 mol% concentration the rare earth ion is found in cubic, trigonal, and tetragonal

¹⁾ 54037 Nancy Cédex, France.

sites. In the cubic site, the F_i ion is far from any R ion, in the tetragonal site the F_i ion is in the nearest neighbour interstitial site (nn), and in the trigonal site the F_i is in the next nearest neighbour interstitial site (nnn).

The rare earth concentrations present in the barium fluoride crystals have been determined by radioactivation (for 0.2 mol%) and X-fluorescence (for 0.4 to 1 mol%) analysis. These measured concentrations are close to the introduced ones.

The spectra are recorded using a grating spectrometer with a bolometer detector [11].

2. Far Infrared Spectra

Fig. 1 gives the evolution of absorption spectra at different concentrations of barium fluoride doped with Dy^{3+} ions (0.20, 0.40, 0.60, 0.77, and 0.98 mol%). The additional absorption caused by the introduction of Dy^{3+} is plotted versus wave number (cm^{-1}).

(i) The absorption increases regularly when the Dy^{3+} concentration increases in the crystal, and the structure of the three bands observed for BaF_2 doped with 0.2 mol% becomes complicated and new peaks appear.

The 75.5 cm^{-1} band ascribed to the longitudinal vibration of the compensation F_i ion in a tetragonal site widens; several lines seem to be responsible for this around 63 and 80 cm^{-1} and two important peaks appear at 53 and 59 cm^{-1} .

In the 131.5 cm^{-1} band we observe four lines. The 131.5 cm^{-1} line observed for any R ion has been attributed to the vibration of the F_i ion in a cubic site. The weak 125 cm^{-1} line observed before in $BaF_2:Nd^{3+}$ and $BaF_2:Ho^{3+}$ has been ascribed to the longitudinal vibration of the F_i ion in a trigonal site. A line appears at 135 cm^{-1} and an inflexion at 120 cm^{-1} . The 135 cm^{-1} line observed for the first time confirms our model and will be discussed later.

The 160 cm^{-1} band has been ascribed to the transverse vibration of the F_i ion in a tetragonal site. Several peaks are detected, their intensity being dependent on the concentration in Dy^{3+} ions. A large number of lines is expected in the area and can explain this fact.

(ii) When the Dy^{3+} ion concentration increases, the 42 cm^{-1} line ascribed to electronic transition of the Dy^{3+} ion in a trigonal site disappears. The fact is remarkable and will be discussed later.

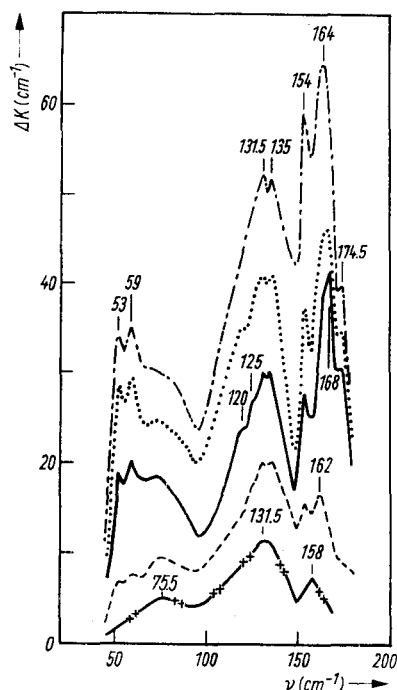


Fig. 1. Additional absorption induced by Dy^{3+} in BaF_2 from 45 to 180 cm^{-1} ; $T = 1.4\text{ K}$. + + + + + 0.20, - - - - 0.40, ——— 0.60, 0.77, and - . - . - 0.98 mol%

(iii) For rare earth concentration higher than 1 mol% FIR absorption becomes too important and in these conditions we cannot study the absorption spectra in the three absorption band areas; besides, in that case, no other line appears in the low frequency area.

3. Discussion

When the Dy^{3+} concentration increases the spectrum complexity seems to show the existence of the several cluster types; this is in agreement with the literature [3 to 10]. Since the three-broad-band absorption structure is preserved, the perturbation terms brought about by the presence of several rare earth ion close to F_i are relatively weak for the frequencies of the F_i ion. This will be confirmed by the model that we propose below. Two facts seem to be remarkable: the presence of the 135 cm^{-1} line and the disappearance of the 42 cm^{-1} line when the Dy^{3+} concentration increases.

In our previous papers we calculated the longitudinal ν_L and transverse ν_T vibrational mode frequencies of the F_i in a trigonal site; we obtained $\nu_L = 125\text{ cm}^{-1}$ and $\nu_T = 135\text{ cm}^{-1}$. The 125 cm^{-1} line was, experimentally, observed only for the Nd^{3+} and Ho^{3+} ions at 0.2 mol% concentration and the 135 cm^{-1} line was never observed for all rare earths introduced. For a concentration equal to or higher than to 0.4 mol% we now observe the 125 cm^{-1} line for the Dy^{3+} ion but, what is more, the 135 cm^{-1} line; this fact seems to confirm our preceding model [1].

The disappearance of the 42 cm^{-1} electronic transition shows that the trigonal site for the Dy^{3+} ion ceases to exist when the concentration of the ion increases; this fact may look paradox since the F_i vibration lines in a nnn site are strengthened; but this fact can be explained by our simple model where the F_i ion symmetry is not the same as that of the rare earth (Fig. 2). Although the lattice constant is high ($a_0 = 6.2\text{ \AA}$), the number of possible sites and the probable presence of deformations does not enable us to propose a serious model. The number of parameters to be determined is very high, the infrared spectrum not being sufficient to achieve full determination, other methods of analysis are necessary to propose a trust worthy model.

Nevertheless we can have a notion of the possible frequencies through the use of simple models, since they will not take into consideration possible deformations, polarisability, and ion effective charge. But their great advantage is to give information on the observed spectra.

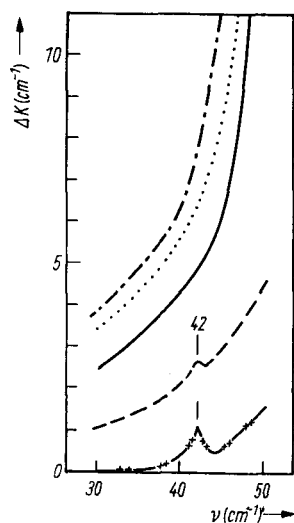


Fig. 2. Additional absorption induced by Dy^{3+} in BaF_2 in 42 cm^{-1} area; $T = 1.4\text{ K}$. + + - + - 0.20, - - - - 0.40, ——— 0.60, 0.77, and - . - . - 0.98 mol%

4. Proposed Models

When the F_i ion is far from any R^{3+} ion we assume a cubic harmonic potential giving ν_c as the vibration frequency. For the other sites we have to add a Coulomb perturbation.

For the $R - F_i - R$ model proposed in Fig. 3, all this leads to the following equation system for the perturbed site:

$$\begin{aligned} 0 &= [\omega^2 - \omega_c^2 + 2A]x + \frac{A}{3} \sqrt{\frac{2}{3}} y, \\ 0 &= \frac{A}{3} \sqrt{\frac{2}{3}} x + \left[\omega^2 - \omega_c^2 - A \left(1 - \frac{1}{3\sqrt{3}} \right) \right] y, \\ 0 &= \omega^2 z - \left[\omega_c^2 + A \left(1 + \frac{1}{3\sqrt{3}} \right) \right] z, \end{aligned}$$

where

$$A = \frac{|qq'|}{4\pi\epsilon_0 m_F} \left(\frac{2}{a} \right)^3$$

and ω and ω_c are the perturbed and cubic pulsations, respectively. The calculation gives $\nu = 58 \text{ cm}^{-1}$, $\nu' = 151 \text{ cm}^{-1}$, and $\nu_z = 160 \text{ cm}^{-1}$. ν and ν' are the vibration frequencies in the $R - F_i - R$ plane, the ν_z vibration axis being perpendicular to it.

In the same hypothesis, the $R - F_{i1} - R - F_{i2}$ model proposed in Fig. 4 gives the following equation system:

$$\begin{aligned} 0 &= \left[\omega^2 - \omega_c^2 + A \left(2 + \frac{1}{16\sqrt{2}} \right) \right] x_1 - \frac{A}{16\sqrt{2}} x_2 + \frac{A}{3} \sqrt{\frac{2}{3}} y_1, \\ 0 &= \frac{A}{3} \sqrt{\frac{2}{3}} x_1 + \left[\omega^2 - \omega_c^2 + A \left(\frac{1}{3\sqrt{3}} - 1 - \frac{1}{8\sqrt{2}} \right) \right] y_1 + \frac{A}{8\sqrt{2}} y_2, \end{aligned}$$

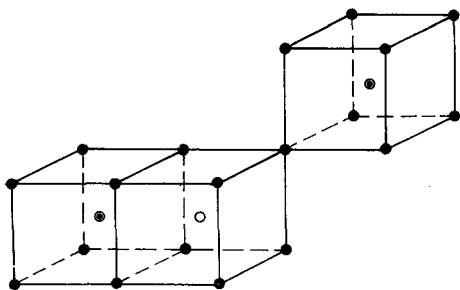


Fig. 3

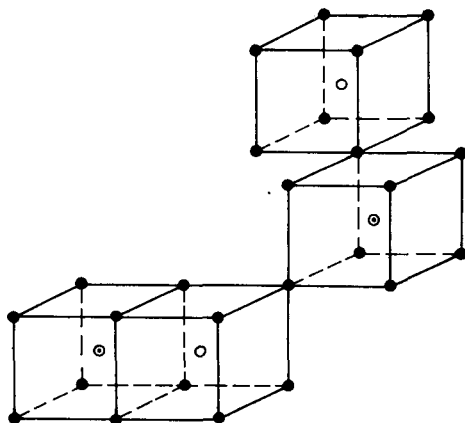


Fig. 4

Fig. 3. First model: BaF_2 lattice with two substitutional rare-earth ions and one charge compensating ion (F_i). $\circ F_i$, $\bullet F^-$, $\circ R^{3+}$

Fig. 4. Second model: BaF_2 lattice with two substitutional rare-earth ions and two charge compensating ions (F_i). Symbols as in Fig. 3

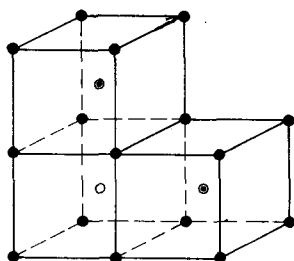


Fig. 5. Third model: BaF₂ lattice with two substitutional rare earth ions situated in nearest neighbour sites and one charge compensating ion (F_i). Symbols as in Fig. 3

$$\begin{aligned}
 0 &= -\frac{A}{16\sqrt{2}}x_1 + \left[\omega^2 - \omega_c^2 + A \left(\frac{1}{16\sqrt{2}} - \frac{2}{81} \right) \right] x_2 + \\
 &\quad + A \left(\frac{2\sqrt{2}}{81} - \frac{1}{3} \sqrt{\frac{2}{3}} \right) y_2, \\
 0 &= A \left(\frac{2\sqrt{2}}{81} - \frac{1}{3} \sqrt{\frac{2}{3}} \right) x_2 + \frac{A}{8\sqrt{2}}y_1 + \\
 &\quad + \left[\omega^2 - \omega_c^2 + A \left(\frac{5}{81} + \frac{1}{3\sqrt{3}} - \frac{1}{8\sqrt{2}} \right) \right] y_2, \\
 0 &= \omega^2 - \omega_c^2 + A \left(\frac{1}{16\sqrt{2}} - 1 - \frac{1}{3\sqrt{3}} \right) z_1 - \frac{A}{16\sqrt{2}}z_2, \\
 0 &= -\frac{A}{16\sqrt{2}}z_1 + \left[\omega^2 - \omega_c^2 + A \left(\frac{1}{16\sqrt{2}} - \frac{1}{27} - \frac{1}{3\sqrt{3}} \right) \right] z_2.
 \end{aligned}$$

The calculation leads to the following frequencies:

$$\begin{aligned}
 \nu_1 &= 54.6 \text{ cm}^{-1}, & \nu'_1 &= 154.0 \text{ cm}^{-1}, & \nu_{z1} &= 158.8 \text{ cm}^{-1}, \\
 \nu_2 &= 122.1 \text{ cm}^{-1}, & \nu'_2 &= 135.4 \text{ cm}^{-1}, & \nu_{z2} &= 136.2 \text{ cm}^{-1}.
 \end{aligned}$$

These vibration frequencies are close to those obtained for the first and for the F_i ion in nnn site.

A third model seems interesting to us (Fig. 5). Still in the same conditions the frequencies are $\nu = \nu' = 102 \text{ cm}^{-1}$ and $\nu_z = 175 \text{ cm}^{-1}$. For this model we have also calculated this frequency with a deformation using a R — F_i — R angle equal to 120°, we find $\nu = \nu' = 83 \text{ cm}^{-1}$.

5. Conclusion

With these few models the spectra are roughly described. On their basis the relative intensities of the different perturbation terms on the tetragonal term can be estimated: in the first R — F_i — R model (Fig. 3) we can easily see that the terms due to the nnn rare earth ion are weak compared with the nn rare earth ion terms and their influence on the vibration frequencies is less than 1%. In the R — F_{i1} — R — F_{i2} model (Fig. 4) obtained by adjunction of one F_i ion to the first model, the F_i ion vibrations are also very little perturbed by the presence of the second ion, since the F_{i1} — F_{i2} distance is large (higher than the lattice constant). In the second model the additional F_i can be placed in different sites, but the calculated frequencies are close; this fact can explain the line widening. These considerations showing the presence of higher clusters can be revealed with difficulty by the FIR method.

The electronic transition at 42 cm^{-1} ascribed to the Dy^{3+} ion in tetragonal site [12] disappears when the concentration increases; but, in the same conditions, the F_1 vibrations are little perturbed in regard to $R - F_1$ trigonal dimer vibrations.

References

- [1] G. VILLERMAIN-LECOLIER, G. MORLOT, P. STRIMER, J.-P. AUBRY, and A. HADNI, *Phys. Rev. B* **15**, 13 (1977).
- [2] J.-P. AUBRY, G. VILLERMAIN-LECOLIER, G. MORLOT, and A. HADNI, *Infrared Phys.* **18**, 347 (1978).
- [3] M. J. WEBER and R. W. BIERIG, *Phys. Rev. A* **134**, 1492 (1964).
- [4] N. E. KASK and L. A. KORNIENKO, *Fiz. tverd. Tela* **9**, 2291 (1967); *Soviet Phys. — Solid State* **9**, 1795 (1968).
- [5] A. K. CHEETHAM, B. E. FENDER, D. STEELE, R. J. M. TAYLOR, and B. T. M. WILLIS, *Solid State Commun.* **8**, 171 (1970).
- [6] D. STEELE, P. E. CHILDS, and B. E. FENDER, *J. Phys. C* **5**, 2677 (1972).
- [7] I. B. AISENBERG, M. S. ORLOV, and A. L. STOLOV, *Fiz. tverd. Tela* **15**, 1860 (1973); *Soviet Phys. — Solid State* **15**, 1240 (1973).
- [8] C. R. A. CATLOW, *J. Phys. C* **6**, 64 (1973); **9**, 1859 (1976).
- [9] D. R. TALLANT, D. S. MOORE, and J. C. WRIGHT, *J. chem. Phys.* **67**, 2897 (1977).
- [10] R. J. BOOTH, M. R. MUSTAPHA and B. R. MCGARVEY, *Phys. Rev. B* **17**, 4150 (1978).
- [11] A. HADNI and P. STRIMER, *Phys. Rev. B* **5**, 4609 (1972).
- [12] M. V. EREMIN, R. K. LUKS, and A. L. STOLOV, *Fiz. tverd. Tela* **12**, 3473 (1970).

(Received July 19, 1979)